Published in final edited form as:
Exp Neurol. 2013 September ; 247: 496–505. doi:10.1016/j.expneurol.2013.01.021.

Loss of GABAergic neurons in the hippocampus and cerebral cortex of *Engrailed-2* null mutant mice: Implications for autism spectrum disorders

Paola Sgadò[1], **Sacha Genovesi**[1,*], **Anna Kalinovsky**[2,*], **Giulia Zunino**[1,*], **Francesca Macchi**[3,‡], **Manuela Allegra**[3], **Elisa Murenu**[4,#], **Giovanni Provenzano**[1], **Prem Prakash Tripathi**[3,§], **Simona Casarosa**[3,4], **Alexandra L. Joyner**[2], and **Yuri Bozzi**[1,3]

[1]Laboratory of Molecular Neuropathology, Centre for Integrative Biology (CIBIO), University of Trento, Italy

[2]Developmental Biology Program, Sloan-Kettering Institute, New York, NY

[3]C.N.R. Neuroscience Institute, Pisa, Italy

[4]Laboratory of Developmental Neurobiology, Centre for Integrative Biology (CIBIO), University of Trento, Italy

Abstract

The homeobox-containing transcription factor Engrailed-2 (En2) is involved in patterning and neuronal differentiation of the midbrain/hindbrain region, where it is prominently expressed. *En2* mRNA is also expressed in the adult mouse hippocampus and cerebral cortex, indicating that it might also function in these brain areas. Genome-wide association studies revealed that *En2* is a candidate gene for autism spectrum disorders (ASD), and mice devoid of its expression (*En2*$^{-/-}$ mice) display anatomical, behavioural and clinical "autistic-like" features. Since reduced GABAergic inhibition has been proposed as a possible pathogenic mechanism of ASD, we hypothesized that the phenotype of *En2*$^{-/-}$ mice might include defective GABAergic innervation in the forebrain. Here we show that the Engrailed proteins are present in postnatal GABAergic neurons of the mouse hippocampus and cerebral cortex, and adult *En2*$^{-/-}$ mice show reduced expression of GABAergic marker mRNAs in these areas. In addition, reduction in parvalbumin (PV), somatostatin (SOM) and neuropeptide Y (NPY) expressing interneurons is detected in the hippocampus and cerebral cortex of adult *En2*$^{-/-}$ mice. Our results raise the possibility of a link between altered function of En2, anatomical deficits of GABAergic forebrain neurons and the pathogenesis of ASD.

Corresponding author: Yuri Bozzi, Laboratory of Molecular Neuropathology, Centre for Integrative Biology (CIBIO), University of Trento Via delle Regole 101, 38123 Mattarello, Trento, Italy., Phone: +39-0461-283651, Fax: +39-0461-283937, bozzi@science.unitn.it.
[‡]F.M. present address: Laboratory of Neurobiology and Gene Therapy, Department of Molecular and Cellular Medicine, K.U. Leuven, Belgium
[#]E.M. present address: Institute of Physiology, Department of Physiological Genomics, Ludwig-Maximilians-Universität (LMU), München, Germany
[§]P.P.T. present address: Department of Experimental Oncology, European Institute of Oncology (IEO), Milan, Italy
[*]These authors equally contributed to this study

Keywords

homeobox transcription factor; inhibition; interneuron; parvalbumin; neurodevelopmental disorder

INTRODUCTION

The homeobox-containing transcription factor Engrailed-2 (En2) is crucially involved in the regionalization, patterning and neuronal differentiation of the midbrain and hindbrain (Cheng et al., 2010; Gherbassi and Simon, 2006; Herrup et al., 2005; Joyner, 1996; Orvis et al., 2012; Sgaier et al., 2007). *En2* is predominantly expressed in the developing mouse mesencephalon (midbrain) and rhombomere 1 (including the cerebellum primordium), starting at the neural plate stage (embryonic day 8.5) and continuing throughout embryonic and postnatal development (Davis and Joyner, 1988; Joyner, 1996; Wilson et al., 2011). We recently showed that *En2* mRNA is also expressed in the adult mouse hippocampus and cerebral cortex (Tripathi et al., 2009), indicating that *En2* may also function in these brain areas through the adult age.

Two single-nucleotide polymorphisms (SNPs) in the human *Engrailed-2* (*EN2*) gene are associated with autism spectrum disorders (ASD) (Benayed et al., 2005; Gharani et al., 2004). More recently, evidence was provided that one of these SNPs (rs1861973, A-C haplotype) was functional: when tested with a luciferase reporter assay in rat, mouse and human cell lines, this SNP markedly affected *EN2* promoter activity (Benayed et al., 2009). Accordingly, mice lacking the homeobox domain of *En2* (*En2*$^{hd/hd}$ mice; Joyner et al., 1991, referred to as *En2*$^{-/-}$) or N-terminal sequence (Millen et al., 1994) have been proposed as models for ASD, due to their complex neurodevelopmental, neuroanatomical and behavioral phenotype. *En2*$^{-/-}$ mice display cerebellar hypoplasia, including a reduced number of Purkinje cells, and a defect in the antero-posterior pattern of cerebellar foliation (Joyner et al., 1991; Kuemerle et al., 1997; Millen et al., 1994, 1995). Altered anatomy of the amygdala has also been reported in *En2*$^{-/-}$ mice (Kuemerle et al., 2007). All these abnormalities resemble some of those reported in ASD patients (reviewed by Dicicco-Bloom et al., 2006). The behavior of *En2*$^{-/-}$ mice is also reminiscent of some features of ASD individuals. Deficits in social behaviors were detected in young *En2*$^{-/-}$ mice, including decreased play and reduced social interactions; locomotor impairment as well as defective spatial learning and memory were also reported in these mice (Brielmaier et al., 2012; Cheh et al., 2006; Gerlai et al., 1996).

In a previous study, we showed that *En2*$^{-/-}$ mice display an increased seizure susceptibility (Tripathi et al., 2009), a clinical feature that is frequently observed in ASD patients (Spence and Schneider, 2009). We attributed this hyperexcitability to a reduced inhibitory innervation onto principal hippocampal neurons of *En2*$^{-/-}$ mice (Tripathi et al., 2009). Recent studies clearly indicated that defective development of γ-aminobutyric acid (GABA)-positive neurons (and subsequent reduced inhibition) might contribute to the pathogenesis of ASD (Chao et al., 2010; Gogolla et al., 2009; Provenzano et al., 2012). To test this hypothesis, we investigated the profile of GABAergic interneurons in the hippocampus and cerebral cortex of adult *En2*$^{-/-}$ mice by using quantitative RT-PCR and immunohistochemistry for interneuron-specific markers. Here we show that adult *En2*$^{-/-}$ mice display a reduced number of GABAergic neurons in the hippocampus and cerebral cortex.

MATERIALS AND METHODS

Animals

Experiments were conducted in conformity with the European Communities Council Directive of 24 November 1986 (86/609/EEC), and approved by the Italian Ministry of Health, Ethics Committee of the University of Trento and Memorial Sloan-Kettering Cancer Center. Animals were housed in a 12 hr light/dark cycle with food and water available *ad libitum*. All surgery was performed under chloral hydrate anesthesia, and all efforts were made to minimize suffering. The generation of *En2*$^{-/-}$ mice was previously described (Joyner et al., 1991). The original *En2* mutants (mixed 129Sv × C57BL/6 and outbred genetic background) were crossed at least five times into a C57BL/6 background. Heterozygous mating (*En2*$^{+/-}$ × *En2*$^{+/-}$) were used to generate the *En2*$^{+/+}$ (wild type, WT) and *En2*$^{-/-}$ littermates used in this study. PCR genotyping was performed according to the protocol available on the Jackson Laboratory website (www.jax.org; mouse strain *En2*^{tm1Alj}). Four week old outbred WT mice were used for immunohistochemical characterization of En1/2 protein expression. For all the other experiments, WT and *En2*$^{-/-}$ age-matched adult littermates (3-5 months old; weight = 25-35 g) mice of both sexes were used.

Immunohistochemistry

Immunohistochemical characterization of postnatal En1 and En2 protein expression was performed on four weeks old and adult WT mice. Brains were fixed by transcardial perfusion with 4% paraformaldehyde followed by 1 hour post-fixation at 4 °C, and 30 μm thick cryosections were collected. Optimal En1/2 staining was obtained on four weeks old mice (n=4; Fig. 1), whereas a weaker signal was obtained in adult mice (not shown). A total of 13 WT and 14 *En2*$^{-/-}$ adult (3-5 months old) littermates were used for immunohistochemical identification of GABAergic interneuron subtypes and morphometric analyses of the hippocampus and somatosensory cortex (see below). Brains were fixed by immersion in 4% paraformaldehyde and coronal sections (50 μm thick) were cut on a vibratome. Serial sections at the level of the dorsal hippocampus were incubated overnight with appropriate antibodies as follows: affinity purified rabbit polyclonal anti-En-homeodomain1 that recognizes En1 and En2 proteins (αEnhd1; 1:100 dilution; Davis et al., 1991; Wilson et al., 2011); anti-parvalbumin (PV) mouse monoclonal (Sigma-Aldrich, USA; 1:2000 dilution); anti-somatostatin (SOM) rabbit polyclonal (Bachem, UK; 1:2000 dilution); anti-neuropeptide Y (NPY) rabbit polyclonal (Bachem, UK; 1:2000 dilution); anti-calbindin 28kD (CALB) mouse monoclonal (Swant, Switzerland; 1:5000 dilution); anti-glutamic acid decarboxylase 67 kDa isoform (GAD67) monoclonal (Millipore, USA; 1:500 dilution). Signals were revealed with biotin-conjugated secondary antibody and streptavidin conjugated to appropriate fluorophores (AlexaFluor 488/594, Invitrogen Life Technologies, USA). For morphometric analysis (see below), sections were probed with anti-NeuN mouse monoclonal (Millipore, USA; 1:500 dilution) antibody and signal was revealed by diaminobenzidine staining. NeuN staining confirmed cerebellar hypoplasia in *En2*$^{-/-}$ brains (not shown), according to previous studies (Joyner et al., 1991; Kuemerle et al., 1997; Millen et al., 1994, 1995).

Morphometric analysis

Bright-field images of the hippocampus and somatosensory cortex were acquired at 10x primary magnification using a Nikon Eclipse 90i microscope and merged using Adobe Photoshop software. Morphometric analysis of hippocampal and cortical layers was performed according to published protocols (Baj et al., 2012) on 3 to 5 NeuN-stained sections per animal, taken at the level of the dorsal hippocampus (n=4 WT and 5 *En2*$^{-/-}$). Brain areas were identified according to Franklin and Paxinos, (1997). The total thickness of

hippocampus and somatosensory cortex measured in WT mice did not differ from that of C57Bl/6 mice, as from published mouse brain atlases (Franklin and Paxinos, 1997; Allen Mouse Brain Atlas, http://mouse.brain-map.org/) (hippocampal total thickness: WT=1192±30 μm, C57Bl/6=1147±76 μm; somatosensory total thickness: WT= 886±15 μm, C57Bl/6=925±50 μm; t-test, $p>0.05$).

In situ hybridization

Brains from 3 WT and 4 *En2*$^{-/-}$ adult mice were rapidly removed and frozen on dry ice. Coronal cryostat sections (20 μm thick) were fixed in 4% paraformaldehyde. Non-radioactive in situ hybridization was performed as previously described (Tripathi et al., 2009) using a mix containing GAD65 (GenBank ID: M72422) and GAD67 (Genbank ID: NM_017007) digoxigenin-labeled riboprobes. Signal was detected by alkaline phosphatase-conjugated anti-digoxigenin antibody followed by alkaline phosphatase staining. The specificity of the results was confirmed by the use of sense riboprobes (not shown).

Cell counts

Counts of GAD65/67 in situ mRNA positive cells in the hilus and somatosensory cortex were performed on 3 sections per animal (n= 3 WT and 4 *En2*$^{-/-}$ mice) taken at the level of the dorsal hippocampus. Brain areas were identified according to Franklin and Paxinos (1997). For each section, bright-field images of the hilus and somatosensory cortex were acquired at 10x primary magnification using a Nikon Eclipse 90i microscope and merged using Adobe Photoshop software.

Three to five immunolabelled sections at the level of the dorsal hippocampus and somatosensory cortex were analyzed per animal (7 WT and 9 *En2*$^{-/-}$ mice). For each section, large images of the hippocampus and cortex were acquired at 20x primary magnification using a Zeiss Axio Observer z1 microscope with a motorized stage. Acquisitions were automatically performed using the MosaiX and Z-Stack modules of the Zeiss AxioVision software (v4.3.1). Five Z-planes for each image were projected into a single sharp one. Fluorescence intensity, exposure time and microscope settings were optimized for each marker and then held constant. Cell counts were then performed on each image using the ImageJ software. To establish a consistent guideline for counting individual cells, only cell densities larger than 5 μm with a clearly visible nucleus were counted. Signals smaller than 5 μm were excluded to avoid counting neurites, nerve terminals, and false signals.

The same counting procedures were then followed for both in situ hypbridization (GAD65/67) and immunohistochemistry (interneuron subtypes) images. To count positive cells in the hilus, the total hilar area was measured excluding the granule cell layer. The total area of the hilus did not differ between WT and *En2*$^{-/-}$ mice (WT, 109780±5032 μm^2; *En2*$^{-/-}$, 100958±2602 μm^2; t-test, $p>0.05$). Cell densities were then plotted as the number of positive cells/0.1 mm^2. For the somatosensory cortex, cell densities were separately counted in superficial (II-III) and deep (V-VI) layers. A counting frame with an area of 200 μm × 600 μm was used. The sampling field was moved systematically through the cortical layer of interest at least three times for each section. CALB-positive interneurons were identified by double-labelling with GAD67. Cell densities in the cerebral cortex were plotted as the number of positive cells/counting area (200 μm × 600 μm). All counts were performed by two independent experimenters blind of genotypes.

Quantitative RT-PCR

Total RNAs were extracted by Trizol© reagent (Invitrogen) from dissected hippocampi and somatosensory cortices from 7 WT and 7 *En2*$^{-/-}$ adult mice. RNAs were DNAse-treated and

purified with RNeasy Mini Kit (Qiagen, USA). cDNA was synthesized from pooled RNAs (2 μg) using the SuperScript® VILO™ (Invitrogen Life Technologies, USA) according to the manufacturer's instructions. Quantitative real-time PCR was performed using a Rotor-gene 6000™ thermal cycler with real-time detection of fluorescence (Corbett Research, Sydney, Australia). Individual PCR reactions were conducted in a volume of 20 μl using the MESA GREEN qPCR kit (Eurogentec SA, Belgium) according to manufacturer's instructions. Mouse mitochondrial ribosomal protein L41 (Mrpl41) was used as a standard for quantification (Tripathi et al., 2009). Primers (MWG, Germany) were designed on different exons to avoid amplification of genomic DNA. Primer sequences are reported in Table 1. Each PCR cycle consisted of denaturation for 10 s at 94 °C, annealing for 20 s at 60 °C and extension for 30 s at 72 °C. The fluorescence intensity of SYBR green I was read and acquired at 72 °C after completion of the extension step of each cycle. PCR conditions for individual primer sets were optimized by varying template cDNA and primer concentration in order to obtain a single PCR product and amplification efficiency >90%. Relative expression values were calculated using Biogazelle QBASE PLUS v1.5 software (Pfaffl, 2001). Mean cycle threshold values from triplicate experiments (Ct) were calculated for each marker and L41, and corrected for PCR efficiency and inter-run calibration, marker/L41 ratios were then calculated for WT and *En2*$^{-/-}$ mice.

Statistical analyses

Statistical analyses were performed by SigmaStat software. Student's t-test or ANOVA followed by appropriate post-hoc test (as indicated) were used (WT vs. *En2*$^{-/-}$), with statistical significance level set at $p<0.05$.

RESULTS

Expression of the Engrailed proteins in the postnatal mouse hippocampus and cerebral cortex

Our previous study detected *En2* mRNA in the postnatal mouse cerebral cortex and hippocampus (Tripathi et al., 2009). Here, using an antibody that recognizes both En1 and En2 proteins (αEnhd1) on serial sagittal sections, we examined the expression pattern of the two Engrailed proteins (En1/2) in the postnatal mouse forebrain. En1/2 immunopositive cells were scattered throughout all layers of the primary somatosensory cortex (Fig. 1A), as well as in frontal, secondary motor, secondary auditory, visual, insular, piriform, amygdalopiriform, and entorhinal areas (data not shown). En1/2 immunopositive cells were also detected in all subfields of the hippocampal formation (CA1, CA2, CA3, hilus and granule cell layer of the dentate gyrus; Fig. 1F,G). As expected, En1/2 staining in all these structures was nuclear, according to the transcriptional activity of the Engrailed proteins (Fig. 1B,H red labeling). The relative strength of the signal detected in the forebrain with the αEnhd1 antibody, however, was several fold lower compared with the robust expression in the midbrain and cerebellum. Double-labeling experiments revealed that the En1/2 proteins were present (although not exclusively) in PV-positive (Fig. 1C, D, I, J) and CALB-positive (Fig. 1C, D, E, K) interneurons, in both the hippocampus and cerebral cortex.

Normal layering of the adult En2$^{-/-}$ hippocampus

We previously showed a reduced staining of GABAergic markers in the hippocampus of adult *En2*$^{-/-}$ mice compared to WT mice; specifically, reduced PV staining was detected in the pyramidal layer, whereas SOM was decreased in the stratum lacunosum moleculare (Tripathi et al., 2009). We therefore performed a morphometric analysis on dorsal hippocampal sections stained for the pan-neuronal marker NeuN to carefully investigate hippocampal layer structure in WT and *En2*$^{-/-}$ mice. A normal anatomical structure of hippocampal layers was detected in both WT and *En2*$^{-/-}$ mice (Fig. 2A). Total hippocampal

thickness did not differ between WT and *En2*$^{-/-}$ mice (WT: 1192±30 μm, n=4; *En2*$^{-/-}$: 1115±28 μm, n=5; p>0.05, t-test), and no difference was detected in hippocampal layer thickness between the two genotypes (Fig. 2B,C; p>0.05, two-way ANOVA followed by Holm-Sidak test). Thus, the decreased GABAergic innervation observed in the *En2*$^{-/-}$ hippocampus (Tripathi et al., 2009) is likely due to specific defects of selected interneuron subtypes and not to a general alteration of hippocampal structure.

Reduced number of selected populations of GABAergic neurons in the hilus of En2$^{-/-}$ mice

These results prompted us to further investigate the anatomical profile of GABAergic interneurons in the hippocampus of WT and *En2*$^{-/-}$ mice. GABAergic interneurons can be distinguished on the basis of specific markers they express (Ascoli et al., 2008; Jinno and Kosaka, 2010; Mátyás et al., 2004; Rudy et al., 2011). We counted the number of GAD-PV-, NPY-, SOM- and CALB-positive interneurons in the hippocampus of WT and *En2*$^{-/-}$ mice. The total number of GABAergic neurons, estimated by GAD65/67 mRNA *in situ* hybridization, was unchanged in the hilus (Fig. 3A,B) and other hippocampal subfields (data not shown) of *En2*$^{-/-}$ mice, as compared to WT littermates. Immunohistochemistry experiments revealed a clear reduction of PV-, NPY-, SOM-but not CALB-positive interneurons in the hilus of *En2*$^{-/-}$ mice, as compared to WT littermates (Fig. 3A). Quantification of immunohistochemistry experiments confirmed a statistically significant reduction of PV, NPY and SOM interneurons in the *En2*$^{-/-}$ hilus (−38%, −14% and −20%, respectively; p<0.05, Student's t-test; Fig. 3C), whereas no difference was detected in the number of CALB interneurons (Fig. 3B). The number of PV-, NPY-, SOM- and CALB-positive interneurons was unchanged in other subfields of the hippocampal formation (data not shown). These results were confirmed by quantitative RT-PCR on total RNAs extracted from the whole hippocampus of WT and *En2*$^{-/-}$ littermates. A statistically significant decrease of NPY (−48%), PV (−25%), SOM (−24%) but not CALB mRNA expression was detected in *En2*$^{-/-}$ mice as compared to WT controls (Fig. 3D; p<0.05, Student's t-test). mRNA expression levels for pan-GABAergic (glutamic acid decarboxylase, GAD67; vesicular GABA transporter, vGAT) and pan-glutamatergic (vesicular glutamate transporter, vGLUT) markers did not change between the two genotypes (Fig. 3D). These data indicate that, in the absence of major hippocampal morphological alterations, the *En2* null mutation results in the selective reduction of PV, NPY, SOM but not CALB hilar interneurons.

Normal layering of the adult En2$^{-/-}$ somatosensory cortex

Our results indicate that the hippocampus and the somatosensory cortex are the brain areas showing the most robust En1/2 immunoreactivity (Fig. 1). We therefore extended our morphometric and histological analyses also to the somatosensory cortex of *En2*$^{-/-}$ adult mice. NeuN immunohistochemistry revealed no gross layering defects in the somatosensory cortex of adult *En2*$^{-/-}$ mice, as compared to WT littermates (Fig. 4A). Accordingly, morphometric analysis showed that the total thickness of the somatosensory cortex (WT, 886±15 μm; *En2*$^{-/-}$, 938±13 μm) as well as the thickness of each cortical layer (Fig. 4B) did not differ between WT and *En2*$^{-/-}$ mice (p>0.05, two-way ANOVA followed by Holm-Sidak test; n=4 WT and 5 *En2*$^{-/-}$). In situ hybridization for cortical layer specific mRNAs (Molyneaux et al., 2007) confirmed these findings (not shown).

Reduced number of selected populations of GABAergic neurons in the somatosensory cortex of En2$^{-/-}$ mice

We then extended our analysis and counted the number of GAD, PV, NPY, SOM and CALB interneurons in the somatosensory cortex of WT and *En2*$^{-/-}$ mice. The number of GAD65/67 positive interneurons was unchanged throughout the somatosensory cortex of *En2*$^{-/-}$ mice, as compared to WT littermates (Fig. 5A,B). The number of PV and SOM

interneurons was reduced in layers II-III of the *En2*$^{-/-}$ cortex, as compared to WT littermates (Fig. 5C). Quantification confirmed a statistically significant reduction of PV (−44%; $p<0.05$, Student's t-test) and SOM (−25%; $p<0.001$, Student's t-test) interneuron number only in the superficial layers (Fig. 5D). Conversely, a significantly reduced number of NPY interneurons was detected in both superficial and deep layers of the *En2*$^{-/-}$ somatosensory cortex, when compared to WT littermates (−30% and −42% in layers II-III and V-VI, respectively; $p<0.05$, Student's t-test; Fig. 5C,D). CALB-expressing GABAergic interneurons represent a subpopulation of CALB-positive cells of the cerebral cortex: pyramidal glutamatergic neurons also express CALB (Celio, 1990; Jinno and Kosaka, 2010). The total number of CALB-expressing neurons throughout all layers of the somatosensory cortex did not vary between WT and *En2*$^{-/-}$ mice (cells/area in layers II/III: WT=178±9, *En2*$^{-/-}$=193±6; cells/area in layers V-VI: WT=60±4, *En2*$^{-/-}$=57±3; $p>0.05$, Student's t-test). The number of CALB-positive interneurons (identified by GAD67/CALB double staining) was also unchanged between the two genotypes (Fig. 5E,F; $p>0.05$, Student's t-test). Quantitative RT-PCR experiments revealed a slightly different profile of GABAergic marker mRNA expression in the somatosensory cortex: a statistically significant decrease of PV mRNA expression (−10%) was detected in *En2*$^{-/-}$ mice as compared to WT littermates (Fig. 5G; $p<0.05$, Student's t-test). NPY and SOM mRNA expression was unchanged, whereas CALB mRNA expression was significantly decreased (−17%; $p<0.01$, Student's t-test) in mutant mice (Fig. 5G). In both regions analyzed, mRNA expression levels for pan-GABAergic (glutamic acid decarboxylase, GAD67; vesicular GABA transporter, vGAT) and pan-glutamatergic (vesicular glutamate transporter, vGLUT) markers did not change between the two genotypes (Fig. 5G).

Table 2 reports a schematic summary of the results obtained for the different interneuron markers in the hippocampus and somatosensory cortex of WT and *En2*$^{-/-}$ littermates. The loss of specific interneuron subpopulations detected by immunohistochemistry is in agreement with the reduced expression of the corresponding GABAergic markers as revealed by quantitative RT-PCR. Taken together, our data show that loss of mouse *En2* results in a decrease of PV, NPY, and SOM interneuron numbers in the hippocampus and somatosensory cortex.

DISCUSSION

In this study, we show that one or both Engrailed homeobox transcription factors are expressed in subsets of PV- and CALB-expressing GABAergic interneurons of the postnatal mouse hippocampus and somatosensory cortex. Inactivation of the *En2* gene by gene targeting results in a partial loss of PV interneurons in the hippocampus and the superficial layers of the somatosensory cortex. In addition, the number of NPY and SOM (but not CALB) interneurons are reduced in the hilus and somatosensory cortex of *En2* null mutants.

Previous studies showed that loss of *En2* markedly reduces neurogenesis in posterior brain areas, including development of inhibitory neurons in the cerebellum. A reduced number (Kuemerle et al., 1997; Orvis et al., 2012) and delayed maturation (Sudarov and Joyner, 2007) of CALB-expressing Purkinjie neurons of the cerebellum was described in *En2*$^{-/-}$ mice, suggesting that the *En2* gene may have a direct effect on the development of this type of inhibitory neurons. Our results expand this notion, demonstrating that *En2* is involved in the development or maintenance of GABAergic interneurons also in forebrain areas. However, the forebrain interneuron subtypes affected by the *En2* null mutation are different from those in the cerebellum. In the hippocampus and somatosensory cortex, *En2* null mutation results in a partial loss of PV, NPY and SOM (but not CALB) interneurons, without affecting the total number of GAD-expressing interneurons, nor the laminar

structure of these brain areas. This indicates that the *En2* mutation has a very selective, region-specific effect on different subpopulations of GABAergic interneurons.

Table 2 summarizes the different expression profiles observed for the different GABAergic markers analyzed in the hippocampus and somatosensory cortex. Immunohistochemistry and mRNA expression data were in good agreement for the hippocampus: partial loss of PV, NPY and SOM interneurons was accompanied by decreased mRNA levels in $En2^{-/-}$ mice, whereas no difference between the two genotypes was detected in CALB mRNA or cell counts. In the somatosensory cortex, PV mRNA levels and PV-immunopositive cells were both reduced in *En2* mutants, whereas a loss of NPY and SOM neurons was not paralleled by lower mRNA expression levels. This discordance could be due to up-regulation of NPY and SOM mRNAs in the remaining interneurons of the $En2^{-/-}$ somatosensory cortex. Indeed, in rodents, NPY and SOM mRNA up-regulation has been detected in the hippocampus as a consequence of prolonged hyperexcitability (Fetissov et al., 2003; Takahashi et al., 2000). This might be the case also for *En2* mutants, that display increased seizure susceptibility (Tripathi et al., 2009). Accordingly, the downregulation of CALB mRNA in the absence of a reduced number of CALB-positive neurons in the $En2^{-/-}$ cortex might be related to hyperexcitability (Sonnenberg et al., 1991).

Our results suggest an unprecedented role of *En2* in the development and/or maintenance of selected populations of GABAergic interneurons of the mouse hippocampus and somatosensory cortex. The *En2* gene has long been known to have a crucial role in pattern formation of the midbrain and hindbrain regions (see references in the Introduction), but recent work suggests that *En2* function is also involved in the development of telencephalic structures, that also express *En2* mRNA (Tripathi et al., 2009) and both Engrailed proteins (this study). An anterior shift of the lateral, basolateral, central and medial nuclei of the amygdala was already reported in $En2^{-/-}$ mice, but no loss of GAD-positive GABAergic neurons was detected in the whole amygdaloid complex is this previous study (Kuemerle et al., 2007). In keeping with these findings, mRNA expression levels for pan-GABAergic markers (GAD67 and vGAT) and the total number of GAD-positive interneurons (Fig. 3 and 5) were unchanged in the hippocampus and somatosensory cortex of $En2^{-/-}$ mice, as compared to WT littermates. Nevertheless, the present study indicates that specific subsets of hippocampal and cortical interneurons (PV, SOM and NPY) are affected in adult *En2* mutants. Many different interneuron populations are present in the adult forebrain (Ascoli et al., 2008; Jinno and Kosaka, 2010; Mátyás et al., 2004). In the cerebral cortex, PV and SOM interneurons account for about 70% of all interneurons (30% PV, 30% SOM, 10% PV +SOM; Rudy et al., 2011). In the hippocampus, PV and SOM interneurons represent the vast majority (90%) of GAD-positive neurons (40% PV, 50% SOM; Tricoire et al., 2011). It is therefore surprising that the partial loss of specific PV, SOM and NPY interneurons does not affect the total number of GABAergic neurons in the $En2^{-/-}$ forebrain. A possible explanation for these findings is that the relative percentages of different interneuron populations are altered in mutant mice, without affecting the total number of GAD-positive neurons. The analysis of other interneuron markers such as serotonin 5HT3a receptor, vasointestinal peptide (VIP) and cholecystokin (CCK) (Rudy et al., 2011, Tricoire et al., 2011) are currently ongoing in our laboratory to address this issue.

It remains to be determined how the *En2* mutation can impact GABAergic interneuron development or maintenance. Studies performed on the development of cerebellar Purkinjie neurons (see references in the Introduction) and mesencephalic dopaminergic neurons (Alavian et al., 2009; Albéri et al., 2004; Sgadò et al., 2006) suggest that the *Engrailed* genes play a crucial role in controlling neuronal survival: for example *Engrailed genes* knockout results in apoptosis of selected neuronal populations arising from the midbrain/hindbrain region. Experiments performed on $En2^{-/-}$ and WT mice expressing GFP-labelled

interneurons are currently ongoing in our laboratory to address the developmental origin of the observed partial loss of GABAergic interneurons in the *En2*$^{-/-}$ hippocampus and cerebral cortex.

Preliminary RNA microarray experiments show that mRNAs encoding for proteins implicated in GABAergic synaptic function (receptors, structural proteins, signaling molecules) are down-regulated in the hippocampus of *En2*$^{-/-}$ adult mice compared to WT littermates (our unpublished observations). Together with the results presented in this study, these observations confirm a significant impairment of GABAergic synaptic function in the *En2*$^{-/-}$ forebrain, and suggest that interneuron deficits might be at the origin of some of the complex behavioural (Cheh et al., 2006; Gerlai et al., 1996) and clinical (Tripathi et al., 2009) phenotypes observed in these mice. Altered or delayed development of GABAergic inhibition has been proposed as a pathogenic mechanism of multiple neurodevelopmental disorders, including ASD (Di Cristo, 2007). A significant reduction of GABAergic inhibitory Purkinje cell neurons of the cerebellum of autistic patients has long been reported (Bauman and Kemper, 2005; Whitney et al., 2008, 2009). More recently, post-mortem studies showed an abnormal density of Calretinin-, CALB- and PV-immunoreactive interneurons in the hippocampus of ASD patients, when compared to control samples (Lawrence et al., 2010). The authors of this study proposed that “GABAergic interneurons may represent a vulnerable target in the brains of individual with autism” (Lawrence et al., 2010). In addition, abnormalities in GABAergic neuron circuitry have been reported in several mouse models of ASD (Provenzano et al., 2012; Sgadò et al., 2011). Specifically, a marked loss of PV-expressing interneurons (a feature that also is observed in *En2*$^{-/-}$ mice) has been detected in the somatosensory cortex of *Fmrp, MeCP2* and *Neuroligin 3* mutants, as well as valproic acid-treated mice (Gogolla et al., 2009).

Structural and functional abnormalities of GABAergic interneurons might represent the anatomical substrate of an unbalanced excitation/inhibition ratio in the cerebral cortex and other brain areas, that has been postulated to occur in the autistic brain (Rubenstein and Merzenich, 2003). Impaired maturation of GABAergic circuitry has been shown to result in an immature function of the cerebral cortex, that remains more plastic and sensitive to alterations in sensory inputs (Hensch, 2005; Di Cristo, 2007). Importantly, altered plasticity of the visual cortex has also been recently reported in mouse models of mental retardation such as *Fmr1* (Dölen et al., 2007) and *MeCP2* (Tropea et al., 2009) mutant mice, thus confirming the idea that an immature structure and function of the cerebral cortex is considered a major feature of neurodevelopmental disorders.

CONCLUSIONS

The reduced number of specific subsets of GABAergic interneurons in the cerebral cortex of *En2*$^{-/-}$ mice might be indicative of an immature cortical connectivity and might account for aspects of the complex behavioural phenotype, as well as increased seizure susceptibility observed in these mutants. Our results strengthen the notion that *En2*$^{-/-}$ mice can be used as a model to further investigate the role of cortical GABAergic interneurons in the pathogenesis of ASD.

Acknowledgments

P.S. is supported by Provincia Autonoma diTrento (Italy) under the Marie Curie-People cofunding action of the European Community. This work was funded by the Italian Ministry of University and Research (PRIN 2008 grant # 200894SYW2_002 to Y.B.), the University of Trento (CIBIO start-up grant to S.C. and Y.B.), and a grant from the National Institutes of Health, USA (MH085726 to A.L.J.). We thank Andrea Messina, Mark Dunleavy (CIBIO, University of Trento, Italy), Enrico Tongiorgi (University of Trieste, Italy), Massimo Pasqualetti (Biology Dept., University of Pisa, Italy), Matteo Caleo (CNR Neuroscience Institute, Pisa, Italy) for helpful discussions and

reagents, and Patrizia Paoli (CIBIO, University of Trento, Italy), Barbara Roncolini, Elena Orsucci (CNR Neuroscience Institute, Pisa, Italy) for administrative support.

Abbreviations

ASD	autism spectrum disorders
CALB	calbindin 28kD
CCK	cholecystokin
DG	dentate gyrus
En2	Engrailed-2
GABA	γ-aminobutyric acid
GAD	glutamic acid decarboxylase
NPY	neuropeptide Y
PV	parvalbumin
RT-PCR	reverse transcrition polymerase chain reaction
SNP	single-nucleotide polymorphism
SOM	somatostatin
vGAT	vesicular GABA transporter
vGLUT	vesicular glutamate transporter
VIP	vasointestinal peptide

REFERENCES

Alavian KN, Sgadò P, Albéri L, Subramaniam S, Simon HH. Elevated P75NTR expression causes death of engrailed-deficient midbrain dopaminergic neurons by Erk1/2 suppression. Neural Dev. 2009; 4:11. [PubMed: 19291307]

Albéri L, Sgadò P, Simon HH. Engrailed genes are cell-autonomously required to prevent apoptosis in mesencephalic dopaminergic neurons. Development. 2004; 131:3229–3236. [PubMed: 15175251]

Ascoli GA, Alonso-Nanclares L, Anderson SA, Barrionuevo G, Benavides-Piccione R, Burkhalter A, Buzsáki G, Cauli B, Defelipe J, Fairén A, et al. Petilla terminology: nomenclature of features of GABAergic interneurons of the cerebral cortex. Nat Rev Neurosci. 2008; 9:557–568. [PubMed: 18568015]

Baj G, D'Alessandro V, Musazzi L, Mallei A, Sartori CR, Sciancalepore M, Tardito D, Langone F, Popoli M, Tongiorgi E. Physical exercise and antidepressants enhance BDNF targeting in hippocampal CA3 dendrites: further evidence of a spatial code for BDNF splice variants. Neuropsychopharmacology. 2012; 37:1600–1611. [PubMed: 22318196]

Bauman ML, Kemper TL. Neuroanatomic observations of the brain in autism: a review and future directions. Int J Dev Neurosci. 2005; 23:183–187. [PubMed: 15749244]

Benayed R, Choi J, Matteson PG, Gharani N, Kamdar S, Brzustowicz LM, Millonig JH. Autism-associated haplotype affects the regulation of the homeobox gene, ENGRAILED 2. Biol Psychiatry. 2009; 66:911–917. [PubMed: 19615670]

Benayed R, Gharani N, Rossman I, Mancuso V, Lazar G, Kamdar S, Bruse SE, Tischfield S, Smith BJ, Zimmerman RA, et al. Support for the homeobox transcription factor gene ENGRAILED 2 as an autism spectrum disorder susceptibility locus. Am J Hum Genet. 2005; 77:851–868. [PubMed: 16252243]

Brielmaier J, Matteson PG, Silverman JL, Senerth JM, Kelly S, Genestine M, Millonig JH, Dicicco-Bloom E, Crawley JN. Autism-relevant social abnormalities and cognitive deficits in engrailed-2 knockout mice. PLoS ONE. 2012; 7:e40914. [PubMed: 22829897]

Celio MR. Calbindin D-28k and parvalbumin in the rat nervous system. Neuroscience. 1990; 35:375–475. [PubMed: 2199841]

Chao H-T, Chen H, Samaco RC, Xue M, Chahrour M, Yoo J, Neul JL, Gong S, Lu H-C, Heintz N, et al. Dysfunction in GABA signalling mediates autism-like stereotypies and Rett syndrome phenotypes. Nature. 2010; 468:263–269. [PubMed: 21068835]

Cheh MA, Millonig JH, Roselli LM, Ming X, Jacobsen E, Kamdar S, Wagner GC. En2 knockout mice display neurobehavioral and neurochemical alterations relevant to autism spectrum disorder. Brain Res. 2006; 1116:166–176. [PubMed: 16935268]

Cheng Y, Sudarov A, Szulc KU, Sgaier SK, Stephen D, Turnbull DH, Joyner AL. The Engrailed homeobox genes determine the different foliation patterns in the vermis and hemispheres of the mammalian cerebellum. Development. 2010; 137:519–529. [PubMed: 20081196]

Davis CA, Joyner AL. Expression patterns of the homeo box-containing genes En-1 and En-2 and the proto-oncogene int-1 diverge during mouse development. Genes Dev. 1988; 2:1736–1744. [PubMed: 2907320]

Davis CA, Holmyard DP, Millen KJ, Joyner AL. Examining pattern formation in mouse, chicken and frog embryos with an En-specific antiserum. Development. 1991; 111:287–298. [PubMed: 1680044]

Di Cristo G. Development of cortical GABAergic circuits and its implications for neurodevelopmental disorders. Clin Genet. 2007; 72:1–8. [PubMed: 17594392]

Dicicco-Bloom E, Lord C, Zwaigenbaum L, Courchesne E, Dager SR, Schmitz C, Schultz RT, Crawley J, Young LJ. The developmental neurobiology of autism spectrum disorder. J Neurosci. 2006; 26:6897–6906. [PubMed: 16807320]

Dölen G, Osterweil E, Rao BSS, Smith GB, Auerbach BD, Chattarji S, Bear MF. Correction of fragile X syndrome in mice. Neuron. 2007; 56:955–962. [PubMed: 18093519]

Fetissov SO, Jacoby AS, Brumovsky PR, Shine J, Iismaa TP, Hökfelt T. Altered hippocampal expression of neuropeptides in seizure-prone GALR1 knockout mice. Epilepsia. 2003; 44:1022–1033. [PubMed: 12887433]

Franklin, KBJ.; Paxinos, G. The Mouse Brain in Stereotaxic Coordinates. Academic Press; 1997.

Gerlai R, Millen KJ, Herrup K, Fabien K, Joyner AL, Roder J. Impaired motor learning performance in cerebellar En-2 mutant mice. Behav Neurosci. 1996; 110:126–133. [PubMed: 8652061]

Gharani N, Benayed R, Mancuso V, Brzustowicz LM, Millonig JH. Association of the homeobox transcription factor, ENGRAILED 2, 3, with autism spectrum disorder. Mol Psychiatry. 2004; 9:474–484. [PubMed: 15024396]

Gherbassi D, Simon HH. The engrailed transcription factors and the mesencephalic dopaminergic neurons. J Neural Transm Suppl. 2006:47–55. [PubMed: 17017508]

Gogolla N, Leblanc JJ, Quast KB, Südhof T, Fagiolini M, Hensch TK. Common circuit defect of excitatory-inhibitory balance in mouse models of autism. J Neurodev Disord. 2009; 1:172–181. [PubMed: 20664807]

Hensch TK. Critical period plasticity in local cortical circuits. Nat Rev Neurosci. 2005; 6:877–888. [PubMed: 16261181]

Herrup K, Murcia C, Gulden F, Kuemerle B, Bilovocky N. The genetics of early cerebellar development: networks not pathways. Prog. Brain Res. 2005; 148:21–27. [PubMed: 15661178]

Jinno S, Kosaka T. Stereological estimation of numerical densities of glutamatergic principal neurons in the mouse hippocampus. Hippocampus. 2010; 20:829–840. [PubMed: 19655319]

Joyner AL. Engrailed, Wnt and Pax genes regulate midbrain--hindbrain development. Trends Genet. 1996; 12:15–20. [PubMed: 8741855]

Joyner AL, Herrup K, Auerbach BA, Davis CA, Rossant J. Subtle cerebellar phenotype in mice homozygous for a targeted deletion of the En-2 homeobox. Science. 1991; 251:1239–1243. [PubMed: 1672471]

Kuemerle B, Gulden F, Cherosky N, Williams E, Herrup K. The mouse Engrailed genes: a window into autism. Behav Brain Res. 2007; 176:121–132. [PubMed: 17055592]

Kuemerle B, Zanjani H, Joyner A, Herrup K. Pattern deformities and cell loss in Engrailed-2 mutant mice suggest two separate patterning events during cerebellar development. J Neurosci. 1997; 17:7881–7889. [PubMed: 9315908]

Lawrence YA, Kemper TL, Bauman ML, Blatt GJ. Parvalbumin-, calbindin-, and calretinin-immunoreactive hippocampal interneuron density in autism. Acta Neurol Scand. 2010; 121:99–108. [PubMed: 19719810]

Mátyás F, Freund TF, Gulyás AI. Immunocytochemically defined interneuron populations in the hippocampus of mouse strains used in transgenic technology. Hippocampus. 2004; 14:460–481. [PubMed: 15224983]

Millen KJ, Hui CC, Joyner AL. A role for En-2 and other murine homologues of Drosophila segment polarity genes in regulating positional information in the developing cerebellum. Development. 1995; 121:3935–3945. [PubMed: 8575294]

Millen KJ, Wurst W, Herrup K, Joyner AL. Abnormal embryonic cerebellar development and patterning of postnatal foliation in two mouse Engrailed-2 mutants. Development. 1994; 120:695–706. [PubMed: 7909289]

Molyneaux BJ, Arlotta P, Menezes JRL, Macklis JD. Neuronal subtype specification in the cerebral cortex. Nat Rev Neurosci. 2007; 8:427–437. [PubMed: 17514196]

Orvis GD, Hartzell AL, Smith JB, Barraza LH, Wilson SL, Szulc KU, Turnbull DH, Joyner AL. The engrailed homeobox genes are required in multiple cell lineages to coordinate sequential formation of fissures and growth of the cerebellum. Dev Biol. 2012; 367:25–39. [PubMed: 22564796]

Pfaffl MW. A new mathematical model for relative quantification in real-time RT-PCR. Nucleic Acids Res. 2001; 29:e45. [PubMed: 11328886]

Provenzano G, Zunino G, Genovesi S, Sgadò P, Bozzi Y. Mutant mouse models of autism spectrum disorders. Dis Markers. 2012 in press [Epub ahead of print].

Rubenstein JLR, Merzenich MM. Model of autism: increased ratio of excitation/inhibition in key neural systems. Genes Brain Behav. 2003; 2:255–267. [PubMed: 14606691]

Rudy B, Fishell G, Lee S, Hjerling-Leffler J. Three groups of interneurons account for nearly 100% of neocortical GABAergic neurons. Dev Neurobiol. 2011; 71:45–61. [PubMed: 21154909]

Sgadò P, Albéri L, Gherbassi D, Galasso SL, Ramakers GMJ, Alavian KN, Smidt MP, Dyck RH, Simon HH. Slow progressive degeneration of nigral dopaminergic neurons in postnatal Engrailed mutant mice. Proc Natl Acad Sci USA. 2006; 103:15242–15247. [PubMed: 17015829]

Sgadò P, Dunleavy M, Genovesi S, Provenzano G, Bozzi Y. The role of GABAergic system in neurodevelopmental disorders: a focus on autism and epilepsy. Int J Physiol Pathophysiol Pharmacol. 2011; 3:223–235. [PubMed: 21941613]

Sgaier SK, Lao Z, Villanueva MP, Berenshteyn F, Stephen D, Turnbull RK, Joyner AL. Genetic subdivision of the tectum and cerebellum into functionally related regions based on differential sensitivity to engrailed proteins. Development. 2007; 134:2325–2335. [PubMed: 17537797]

Sonnenberg JL, Frantz GD, Lee S, Heick A, Chu C, Tobin AJ, Christakos S. Calcium binding protein (calbindin-D28k) and glutamate decarboxylase gene expression after kindling induced seizures. Brain Res Mol Brain Res. 1991; 9:179–190. [PubMed: 1709439]

Spence SJ, Schneider MT. The role of epilepsy and epileptiform EEGs in autism spectrum disorders. Pediatr Res. 2009; 65:599–606. [PubMed: 19454962]

Sudarov A, Joyner AL. Cerebellum morphogenesis: the foliation pattern is orchestrated by multi-cellular anchoring centers. Neural Dev. 2007; 2:26. [PubMed: 18053187]

Takahashi Y, Tsunashima K, Sadamatsu M, Schwarzer C, Amano S, Ihara N, Sasa M, Kato N, Sperk G. Altered hippocampal expression of neuropeptide Y, somatostatin, and glutamate decarboxylase in Ihara's epileptic rats and spontaneously epileptic rats. Neurosci Lett. 2000; 287:105–108. [PubMed: 10854723]

Tricoire L, Pelkey KA, Erkkila BE, Jeffries BW, Yuan X, McBain CJ. A blueprint for the spatiotemporal origins of mouse hippocampal interneuron diversity. J Neurosci. 2011; 31:10948–10970. [PubMed: 21795545]

Tripathi PP, Sgado P, Scali M, Viaggi C, Casarosa S, Simon HH, Vaglini F, Corsini GU, Bozzi Y. Increased susceptibility to kainic acid-induced seizures in Engrailed-2 knockout mice. Neuroscience. 2009; 159:842–849. [PubMed: 19186208]

Tropea D, Giacometti E, Wilson NR, Beard C, McCurry C, Fu DD, Flannery R, Jaenisch R, Sur M. Partial reversal of Rett Syndrome-like symptoms in MeCP2 mutant mice. Proc Natl Acad Sci U S A. 2009; 106:2029–2034. [PubMed: 19208815]

Whitney ER, Kemper TL, Bauman ML, Rosene DL, Blatt GJ. Cerebellar Purkinje cells are reduced in a subpopulation of autistic brains: a stereological experiment using calbindin-D28k. Cerebellum. 2008; 7:406–416. [PubMed: 18587625]

Whitney ER, Kemper TL, Rosene DL, Bauman ML, Blatt GJ. Density of cerebellar basket and stellate cells in autism: evidence for a late developmental loss of Purkinje cells. J Neurosci Res. 2009; 87:2245–2254. [PubMed: 19301429]

Wilson SL, Kalinovsky A, Orvis GD, Joyner AL. Spatially restricted and developmentally dynamic expression of engrailed genes in multiple cerebellar cell types. Cerebellum. 2011; 10:356–372. [PubMed: 21431469]

HIGHLIGHTS

- Mice lacking the Engrailed 2 gene are a model for autism spectrum disorders
- We show a loss of hippocampal and cortical GABAergic interneurons in En2 null mice
- We propose a link between altered function of En2, GABAergic dysfuction and autism

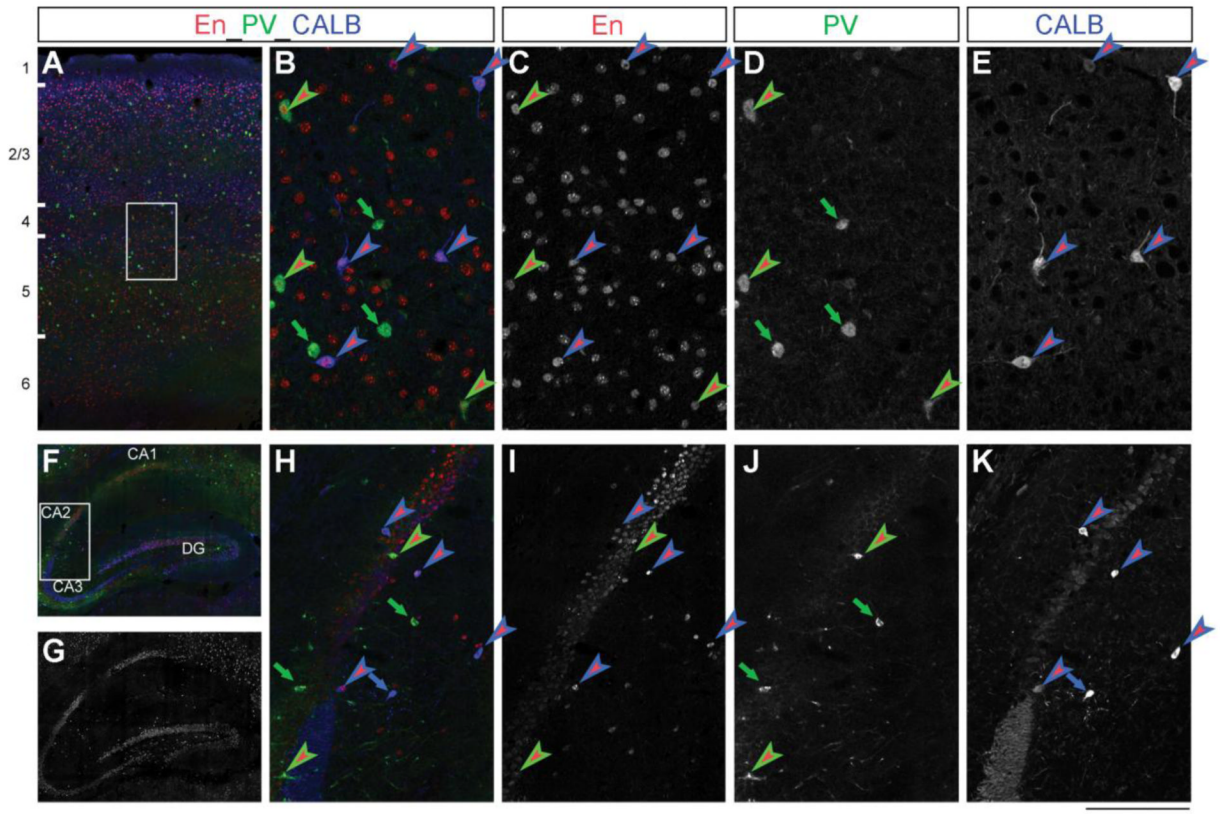

Figure 1. En1/2 proteins are expressed in the postnatal mouse hippocampus and somatosensory cortex

A,B) Triple immunostaing showing En- (red), PV- (green) and CALB- (blue) positive cells in the P28 mouse somatosensory cortex. C,D,E) Single-channel acquisitions of En, PV and CALB immunostains in deep cortical layer (detail of inset shown in A). F,G,H) Triple immunostaing showing En (red), PV (green) and CALB (blue) positive cells in the P28 mouse hippocampus. I,J,K) Single-channel acquisitions of En, PV and CALB immunostainings from the CA2-CA3 boundary (detail of inset shown in G). In all pictures, green-red arrowheads indicate PV-En double positive neurons, and blue-red arrowheads show CALB-En double positive neurons. Green and blue arrows represent PV and CALB neurons not expressing En. Abbreviations: En, Engrailed1/2; PV, parvalbumin; CALB, calbindin; DG, dentate gyrus; CA1-3, hippocampal pyramidal cell layer 1-3. Cortical layers are indicated in A). Scale bar: 400 μm (A), 700 μm (F,G); 95 μm (B-E); 160 μm (H-K).

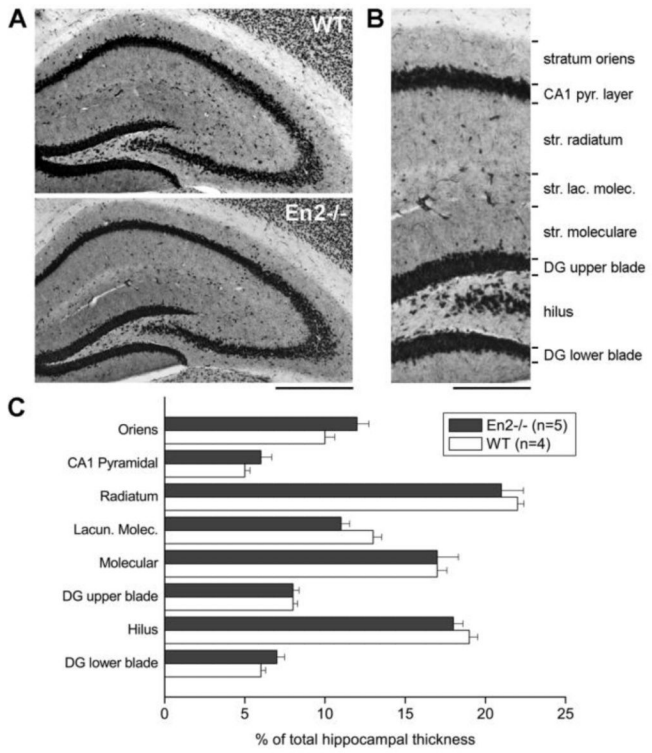

Figure 2. Normal layering of the En2$^{-/-}$ hippocampus

A) Representative NeuN immunostaining of the whole dorsal hippocampus from WT and *En2*$^{-/-}$ mice. B) Subdivision of hippocampal layers used for morphometric analyses. C) Morphometric analysis of hippocampal layers in WT and *En2*$^{-/-}$ mice. Layer thickess is plotted as % of dorsal hippocampus total thickness. Animal numbers and genotypes are as indicated. Abbreviations: DG, dentate gyrus; Lacun. Molec., stratum lacunosum moleculare. NeuN, pan-neuronal marker NeuN. Scale bars: 800 μm (A), 300 μm (B).

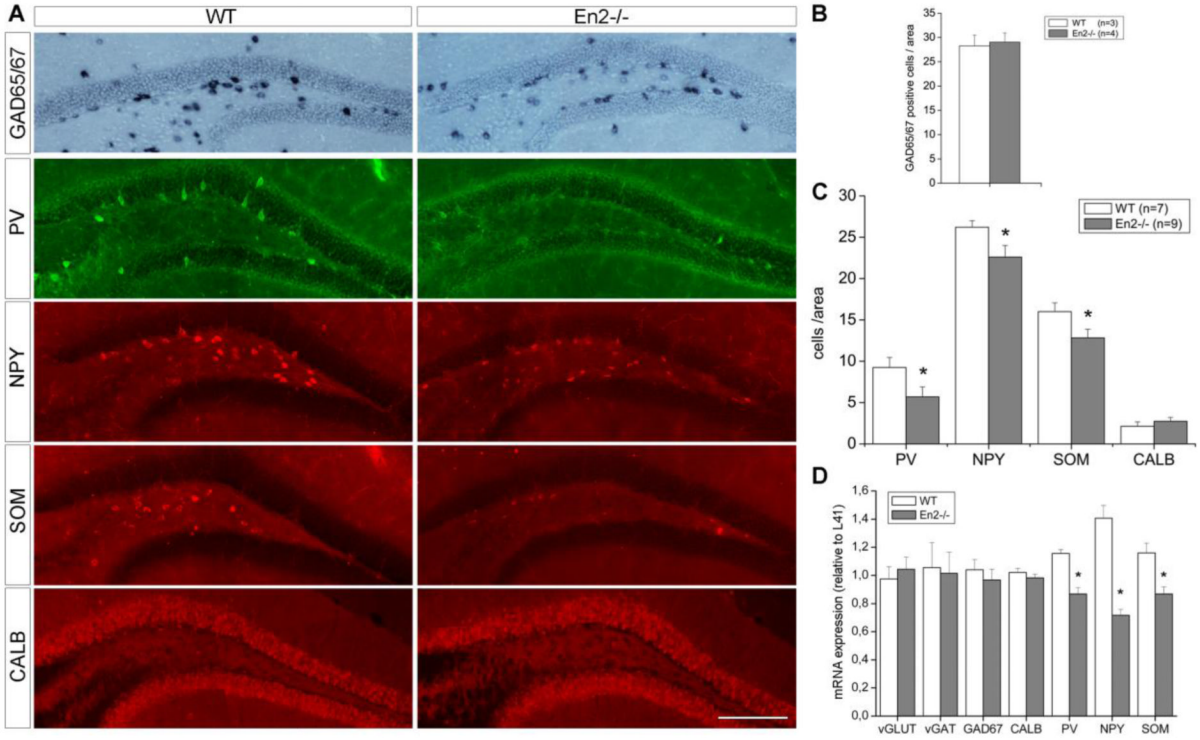

Figure 3. Reduced number of PV, NPY and SOM interneurons in the En2$^{-/-}$ hilus

A) Representative pictures showing GAD-, PV-, NPY-, SOM- and CALB-positive interneurons in the hilus of adult WT and *En2*$^{-/-}$ mice. B) GAD-positive hilar interneuron cell counts. Values are expressed as the mean number (± s.e.m) of positive cells per area (0.1 mm^2, see Material and Methods). C) Subtype-specific hilar interneuron cell counts. Values are reported as in B). Animal numbers and genotypes are as indicated. Asterisk indicates statistical significance (*p< 0.05, Student's t-test, WT *vs. En2*$^{-/-}$). D) Relative mRNA expression level of glutamatergic and GABAergic markers, as obtained by quantitative RT-PCR performed on the whole hippocampus of adult WT and *En2*$^{-/-}$ mice. Values are expressed as each marker/L41 comparative quantitation ratios (mean ± s.e.m of 3 replicates from pools of 7 animals per genotype; *p< 0.05, **p< 0.01, Student's t-test, WT *vs. En2*$^{-/-}$). Abbreviations: vGLUT, vesicular glutamate transporter; vGAT, vesicular GABA transporter; GAD65/67, glutamic acid decarboxylase (65/67 kD isoform); PV, parvalbumin; CALB, calbindin; NPY, neuropeptide Y; SOM, somatostatin. Scale bar: 300 μm.

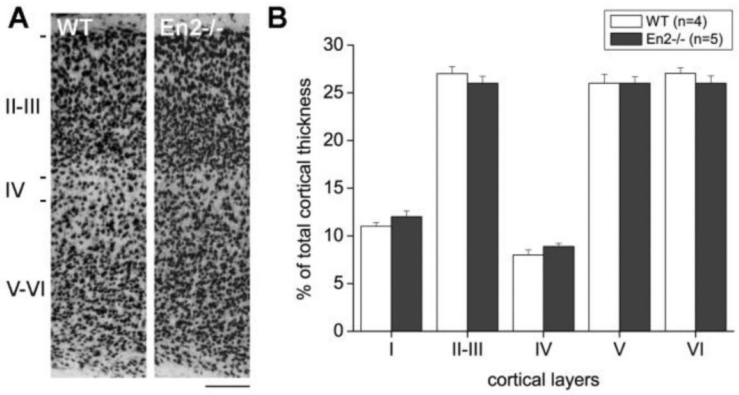

Figure 4. Normal layering of the En2$^{-/-}$ somatosensory cortex

A) Representative NeuN immunostaining of the somatosensory cortex from adult WT and *En2*$^{-/-}$ mice. B) Morphometric analysis of cortical in WT and *En2*$^{-/-}$ mice. Layer thickess is plotted as % of total cortical thickness. Layers, animal numbers and genotypes are as indicated. Scale bar: 120 μm.

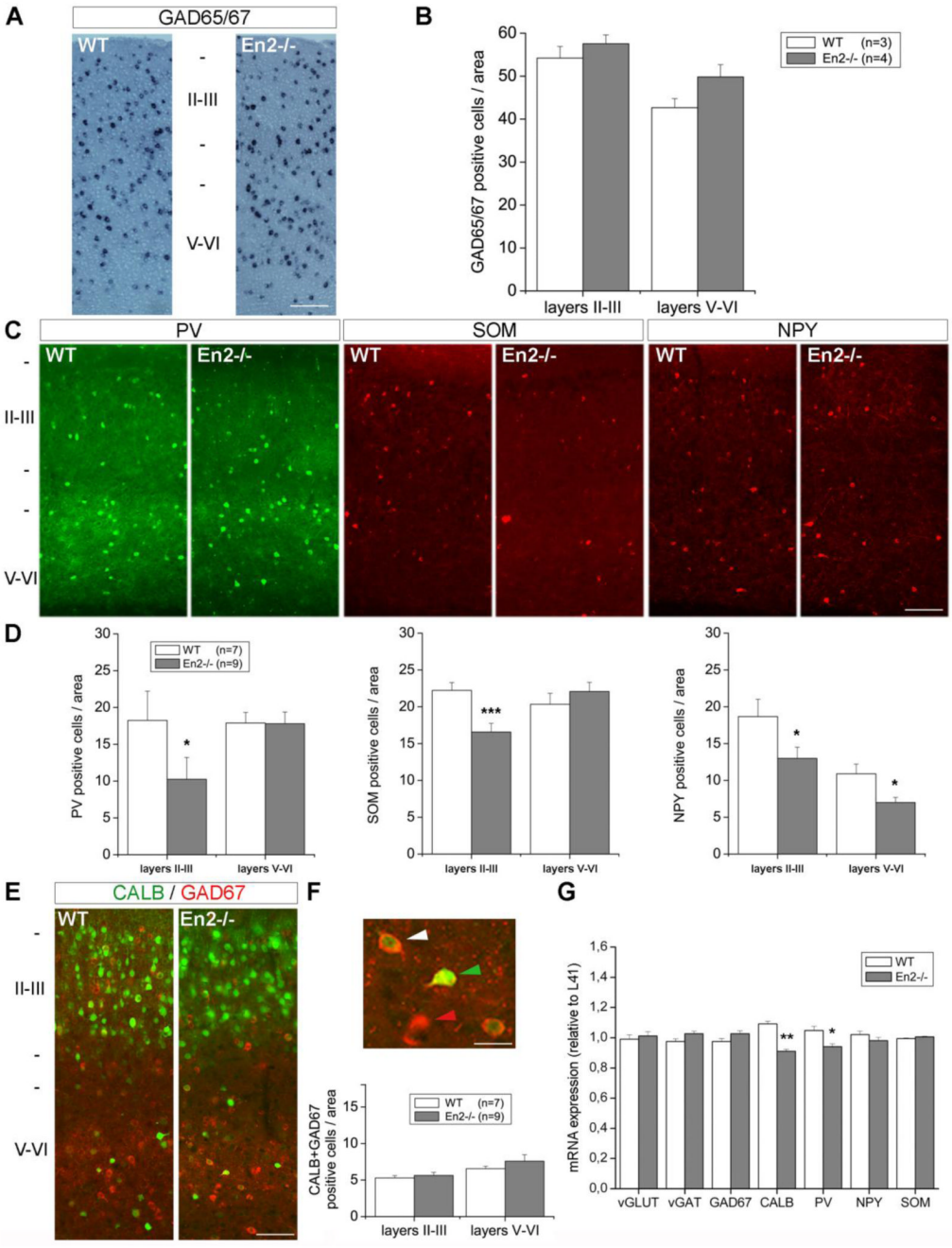

Figure 5. Reduced number of GABAergic interneurons in the En2$^{-/-}$ somatosensory cortex

A) Representative in situ hybridizations showing GAD65/67 mRNA-positive neurons in the somatosensory cortex of adult WT and *En2*$^{-/-}$ mice. B) GAD65/67 mRNA-positive interneuron cell counts. Values are expressed as the mean number (± s.e.m) of positive cells per area (0.12 mm^2, see Material and Methods). C) Representative immunostainings of PV, NPY and SOM interneurons in the somatosensory cortex of adult WT and *En2*$^{-/-}$ mice. D) PV, NPY and SOM interneuron cell counts (values are reported as in B). E) Representative immunostainings of CALB (green) and GAD (red) positive neurons in the somatosensory cortex of adult WT and *En2*$^{-/-}$ mice. F) Top: representative GAD (red arrowhead), CALB (green arrowhead) and GAD+CALB (white arrowhead) interneurons in layers V-VI of the

En2$^{-/-}$ somatosensory cortex. Bottom: cell counts of CALB/GAD double-positive interneurons in the somatosensory cortex of adult WT and *En2*$^{-/-}$ mice (values are reported as in B). G) Relative expression of glutamatergic and GABAergic markers mRNAs in the somatosensory cortex of adult WT and *En2*$^{-/-}$ mice (quantitative RT-PCR). Values are plotted as the mean ± s.e.m of 3 replicates from pools of 7 animals per genotype. In all pictures, abbreviations are as in Fig. 3 and animal numbers, genotypes and cortical layers are as indicated. In all graphs, asterisks indicate statistical significance (*p< 0.05, ***p< 0.001, Student's t-test, WT *vs.* *En2*$^{-/-}$). Scale bars: 200 μm (A), 85 μm (C,E), 20 μm (F).

Table 1
Primers used for quantitative RT-PCR experiments

Gene name	Genbank #	Forward primer (5′-3′)	Reverse primer (5′-3′)
L41	NM_001031808.2	GGTTCTCCCTTTCTCCCTTG	GCACCCCGACTCTTAGTGAA
vGLUT	NM_182993	CACAGAAAGCCCAGTTCAAC	CATGTTTAGGGTGGAGGTAGC
vGAT	NM_009508	TCACGACAAACCCAAGATCAC	GTCTTCGTTCTCCTCGTACAG
GAD67	NM_008077	TCCAAGAACCTGCTTTCCTG	GAGTATGTCTACCACTTCCAGC
CALB	NM_009788	AGATCTGGCTTCATTTCGACG	TTCATTTCCGGTGATAGCTCC
PV	NM_013645	TGCTCATCCAAGTTGCAGG	GCCACTTTTGTCTTTGTCCAG
NPY	NM_023456	TCACAGAGGCACCCAGAG	AGAGATAGAGCGAGGGTCAG
SOM	NM_009215	AGGACGAGATGAGGCTGG	CAGGAGTTAAGGAAGAGATATGGG

Abbreviations as in the text.

Table 2

Reduced expression of interneuron markers and reduced number of interneurons in the hippocampus and somatosensory cortex of *En2*$^{-/-}$ adult mice.

Interneuron marker	Hippocampus		Somatosensory cortex		
	mRNA	**cell counts *(hilus)***	**mRNA**	**cell counts *(layers II-III)***	**cell counts *(layers V-VI)***
GAD	no difference	no difference	no difference	no difference	no difference
PV	−25%	−38%	−10%	−44%	no difference
NPY	−48%	−14%	no difference	−30%	−42%
SOM	−24%	−20%	no difference	−25%	no difference
CALB	no difference	no difference	−17%	no difference	no difference

Data are presented as the mean percentage of the reduction of interneuron marker mRNA and positive cells detected in *En2*$^{-/-}$ mice, as compared to WT littermates. See text and figures for experimental details. Abbreviations as in the text.

Exp Neurol. Author manuscript; available in PMC 2014 September 01.